Numerical investigation of the decay rate of solutions to models for water waves with nonlocal viscosity

Serge Dumont, Jean-Baptiste Duval

NUMERICAL INVESTIGATION OF THE DECAY RATE OF SOLUTIONS TO MODELS FOR WATER WAVES WITH NONLOCAL VISCOSITY

SERGE DUMONT AND JEAN-BAPTISTE DUVAL

Abstract. In this article, we investigate the decay rate of the solutions of two water wave models with a nonlocal viscous term written in the KdV form

$$u_t + u_x + \beta u_{xxx} + \frac{\sqrt{\nu}}{\sqrt{\pi}} \int_0^t \frac{u_t(s)}{\sqrt{t-s}} ds + uu_x = \nu u_{xx}.$$

and

$$u_t + u_x - \beta u_{txx} + \frac{\sqrt{\nu}}{\sqrt{\pi}} \int_0^t \frac{u_t(s)}{\sqrt{t-s}} ds + uu_x = \nu u_{xx}.$$

in the BBM form. In order to realize this numerical study, a numerical scheme based of the G^α-scheme is developed.

Key words. waterwaves, viscous asymptotical models, long-time asymptotics, fractional derivatives.

1. Introduction

Modeling the effect of viscosity on the gravity waves is a challenging issue and much research on this subject has been carried out during last decade. After the pionneer work of Kakutani and Matsuuchi [14], P. Liu and T. Orfila [15], and D. Dutykh and F. Dias [12] have derived, independently, asymptotical models for long gravity waves on viscous shallow water. These models are Boussinesq type systems with a non local in time viscous terms. A one-way reduction of these models was adressed in [11].

Computing the decay rate for solutions of that type of problem is also a challenging issue [1, 3, 4, 8]. In a previous work [7], Chen et *al.* were concerned with computing both theoretically and numerically the decay rate of solutions to a water wave model with a nonlocal viscous dispersive term. This model is the following

$$u_t + u_x + \beta u_{xxx} + \frac{\sqrt{\nu}}{\sqrt{\pi}} \int_0^t \frac{u_t(s)}{\sqrt{t-s}} ds + \gamma uu_x = \alpha u_{xx}, \tag{1}$$

where u is the horizontal velocity of the fluid. This equation requires some comments: the usual diffusion is $-\alpha u_{xx}$, while βu_{xxx} is the geometric dispersion and $\frac{\sqrt{\nu}}{\sqrt{\pi}} \int_0^t \frac{u_t(s)}{\sqrt{t-s}} ds$ stands for the nonlocal diffusive-dispersive term and models the viscosity. Here α, β, γ and ν are non negative parameters dedicated to balance or unbalance the effects of viscosity and dispersion versus the nonlinear effects. Specifically the authors have obtained the following global existence and decay results

The authors thank Professor Olivier Goubet for his pertinent remarks. The present work was initiated when the authors were visiting the Math Department in Purdue University, with the support of the CNRS for the research exchange program *waterwaves*.

for the problem (1) with $\beta = 0$ (see also [13] for $\beta = 1$ and $\gamma = \alpha = 0$) with small initial datum. More precisely, they state the following theorem.

Theorem 1 (Chen et al., 2009)**.** *Consider* (1) *with* $\beta = 0$ *supplemented with initial data* $u_0 \in L^1(\mathbb{R}) \cap L^2(\mathbb{R})$. *There exists* $\epsilon > 0$, $C(u_0) > 0$ *such that for all* $\|u_0\|_{L^1(\mathbb{R})} < \epsilon$, *there exists a unique global solution* $u \in C(\mathbb{R}_+; L^2_x(\mathbb{R})) \cap C^1(\mathbb{R}_+; H_x^{-2}(\mathbb{R}))$. *In addition,* u *satisfies*

$$t^{\frac{1}{2}} \|u(t)\|_{L^\infty_x(\mathbb{R})} + t^{\frac{1}{4}} \|u(t)\|_{L^2_x(\mathbb{R})} \leqslant C(u_0) \tag{2}$$

and u *solves the fixed point equation*

$$u(t,x) = K(t,.) \star u_0 + N * u^2, \tag{3}$$

where K *and* N *are given by*

$$K(t,x) = \frac{1}{2\sqrt{\pi t}}\, e^{-\frac{x^2}{4t}} e^{-x^-} \left(1 + \frac{1}{2}\int_0^{+\infty} e^{-\frac{\mu^2}{4t} - \frac{\mu|x|}{2t} - \frac{\mu}{2}}\, d\mu\right)$$

and

$$N(t,x) = \frac{1}{2\sqrt{\pi t}}\, \partial_x \left[e^{-\frac{x^2}{4t} - x^-} \left(1 - \frac{1}{2}\int_0^{+\infty} e^{-\frac{\mu^2}{4t} - \frac{\mu|x|}{2t} - \frac{\mu}{2}}\, d\mu\right)\right],$$

with $x^- = \max(-x, 0)$, $\star$ *denotes the usual convolution product in space and* $*$ *the time-space convolution product defined by*

$$v * w(t,x) = \int_0^t \int_{\mathbb{R}} v(s,y)\, w(t-s, x-y)\, dx\, dy$$

whenever the integrals make sense.

The proof of this theorem can be found in [7].

We also consider the following equivalent BBM (Benjamin-Bona-Mahony) form of the equation (1)

$$u_t + u_x - \beta u_{txx} + \frac{\sqrt{\nu}}{\sqrt{\pi}} \int_0^t \frac{u_t(s)}{\sqrt{t-s}} ds + \gamma u u_x = \alpha u_{xx}. \tag{4}$$

In this article we investigate the asymptotical decay rate of the solutions with several numerical simulations for the two asymptotic models (1) and (4). First, we will compare our numerical simulations to the results of theorem 1 and those from [7] in order to validate the numerical scheme developed in this article. Then, we will discuss in the sequel the role of respectively the non local viscous terms, the geometric dispersion and the nonlinearity.

This article is organized as follows. In the second section, we recall some definitions and give some notations used in this article, such as the Fourier transform and the Gear operator which will be used to approximate the non local viscous term $\frac{\sqrt{\nu}}{\sqrt{\pi}} \int_0^t \frac{u_t(s)}{\sqrt{t-s}} ds$. In section 3, after a presentation of the numerical scheme, we perform several numerical simulations for equation (1). In the last section, we numerically analyze the decay rate of the solutions for equations (4) with different values of the parameters (α, β, γ and ν).

2. Some notations and definitions

2.1. Notations. Let us introduce some notations that we shall use in the sequel. The Fourier transform of a function u in $L^1(\mathbb{R})$ reads

$$\hat{u}(\xi) = \mathcal{F}(u)(\xi) = \int_{\mathbb{R}} u(x)\, e^{-ix\xi}\, dx.$$

We expect the decay rate of the solution to be $O(t^a)$, with $a < 0$, namely $||u(t,.)||_{L^2_x} \approx Ct^a$ or $||u(t,.)||_{L^\infty_x} \approx Ct^{a'}$ for t large, the ratios

$$R_2 = \frac{\log\left(\frac{||u(t+\Delta t,.)||_{L^2_x}}{||u(t,.)||_{L^2_x}}\right)}{\log(\frac{t+\Delta t}{t})} \quad \text{and} \quad R_\infty = \frac{\log\left(\frac{||u(t+\Delta t,.)||_{L^\infty_x}}{||u(t,.)||_{L^\infty_x}}\right)}{\log(\frac{t+\Delta t}{t})}$$

approach a and a' as $t \to \infty$. Here Δt denotes the time step. We use, in the sequel, the ratios R_2 and R_∞ to describe the decay rate of the solutions.

2.2. Outline of the G^α-scheme. In [7], the time dependent equation

$$u_t + \frac{\sqrt{\nu}}{\sqrt{\pi}} \int_0^t \frac{u_t(s)}{\sqrt{t-s}} ds = f(t), \quad u(t=0) = u_0, \tag{5}$$

is discretized writting u as a convolution

$$u(t) = u_0 + \int_0^t N(\nu(t-s)) f(s)\ ds \tag{6}$$

where $N(t) = \dfrac{1}{\sqrt{\pi}} e^t \displaystyle\int_t^{+\infty} \frac{e^{-s}}{\sqrt{s}}\ ds$. The drawback of this method is that this is not suitable to approximate the solution of equation (4). Then, we consider in this article a direct discretization of the half derivative $\dfrac{1}{\sqrt{\pi}} \displaystyle\int_0^t \frac{u_t(s)}{\sqrt{t-s}} ds$ using the G^α-scheme.

This method consists in approximating the fractional derivative by an Euler backward formula and was developed by Galucio et al [9] (see also [10] for more details). In order to explain the main ideas of this method, let u be a time dependent function, and consider only its discretized values u^n at each time $t^n = n\Delta t$ where n is a positive integer and Δt is the time step, supposed to be fixed. Let G be the Gear operator that approximates the first derivative of u, defined by

$$G = \frac{1}{\Delta t}\left[\frac{3}{2} I - 2\delta^- + \frac{1}{2}(\delta^-)^2\right] \tag{7}$$

where the backward operator δ is defined by

$$(\delta^- u)^n = u^{n-1}.$$

Thus we can formally approximate the α-derivative of u by the formula

$$G^\alpha = \frac{1}{\Delta t^\alpha}\left(\frac{3}{2}\right)^\alpha \left[I - \frac{4}{3}\delta^- + \frac{1}{3}(\delta^-)^2\right]^\alpha. \tag{8}$$

This operator is directly obtained by evaluating the α-power of equation (7). Thus the equation (8) becomes, using the Newton binomial formula:

$$G^\alpha = \frac{1}{\Delta t^\alpha}\left(\frac{3}{2}\right)^\alpha \sum_{j=0}^{\infty}\sum_{l=0}^{j} \left(\frac{4}{3}\right)^j \left(\frac{1}{4}\right)^l (-1)^j\, C_\alpha^j\, (-1)^l\, C_j^l\, (\delta^-)^{j+l},$$

then the α-derivative of u at time t^n can be approximated by

$$(G^\alpha u)^n = \frac{1}{\Delta t^\alpha}\left(\frac{3}{2}\right)^\alpha \sum_{j=0}^{\infty}\sum_{l=0}^{j} \left(\frac{4}{3}\right)^j \left(\frac{1}{4}\right)^l A_{j+1}^\alpha B_{l+1}^j u^{n-j-l} \tag{9}$$

where the coefficients A_{j+1}^δ and B_{l+1}^j are computed using the recurrence formulae:

$$A_{j+1}^\alpha = \frac{j-\alpha-1}{j} A_j^\alpha \quad \text{and} \quad B_{l+1}^j = \frac{l-j-1}{l} B_l^j$$

with $A_1^\alpha = 1$ for any α and $B_1^j = 1$ for any j. For sake of simplicity, we will write in the following the approximation (9) using the expression:

$$(G^\alpha u)^n = \frac{1}{\Delta t^\alpha}\left(\frac{3}{2}\right)^\alpha \sum_{j=0}^{\infty} g_{j+1}^\alpha u^{n-j} \tag{10}$$

where g_{j+1}^α are rational numbers. For numerics, (10) is convenient to approximate the fractional derivatives. Either in equation (1) or in equation (4), the viscous term $\frac{1}{\sqrt{\pi}}\int_0^t \frac{u_t(s)}{\sqrt{t-s}}ds$ will be handled with (10) and $\alpha = 1/2$.

For illustrative purposes, we present in Table 1 the first five coefficients $(g_j^\alpha)_{j=1..5}$ of G^α for three values of α: $\frac{1}{3}$, $\frac{1}{2}$ and $\frac{3}{4}$.

TABLE 1. First five coefficients g_{j+1} of the formal power series (10).

j	$\alpha = 1/3$	$\alpha = 1/2$	$\alpha = 3/4$
0	1	1	1
1	$-\frac{4}{9}$	$-\frac{2}{3}$	-1
2	$-\frac{7}{81}$	$-\frac{1}{18}$	$\frac{1}{12}$
3	$-\frac{104}{2187}$	$-\frac{1}{27}$	$-\frac{1}{108}$
4	$-\frac{643}{19683}$	$-\frac{17}{648}$	$-\frac{1}{96}$
5	$-\frac{4348}{177147}$	$-\frac{19}{972}$	$-\frac{7}{864}$

3. Numerical computation for the KdV-like equation

3.1. The scheme. In this section, we will consider the KdV equation with non local viscosity (1).

The numerical computations on this equation allow us to observe the effect of each term, namely the viscous diffusion, the geometric dispersion and the nonlinearity.

We consider a large interval of $\mathbb{R}$ and we work with periodic boundary conditions in space. The space approximation of the solutions was performed by standard Fourier methods. Since we perform the numerics with an initial data that provides a wave that moves to the right boundary, we expect our computations to be physically relevant until this wave reaches the right boundary.

We now develop the time discretization of the equation (1). Let us introduce a time step $\Delta t > 0$ and set $t_n = n\Delta t$, $\forall\, 0 \le n \le N$, we will denote by u^n the approximate value of $u(t_n)$. We firstly approximate the term u_t as follows:

$$\frac{\partial u}{\partial t} \simeq \frac{u(t_{n+1}) - u(t_n)}{\Delta t} \simeq \frac{u^{n+1} - u^n}{\Delta t}.$$

Thus, using the approximation of the fractional derivative based on the Gear scheme developed in the previous section, the discretization in time of the equation

(1) reads

$$\begin{aligned}(11)\qquad &\frac{u^{n+1}-u^n}{\Delta t}+\frac{\sqrt{\nu}}{\sqrt{\Delta t}}\sqrt{\frac{3}{2}}\sum_{j=0}^{n} g_{n+1-j}u^{j+\frac{1}{2}}\\ &\qquad = \alpha u_{xx}^{n+\frac{1}{2}} - u_x^{n+\frac{1}{2}} - \beta u_{xxx}^{n+\frac{1}{2}} - \gamma\frac{1}{2}(u^n)_x^2,\end{aligned}$$

where $u^{j+\frac{1}{2}} = \frac{1}{2}(u^j + u^{j+1})$, $0 \le j \le n$. Finally applying a Fourier transform in space to the equation (11), we obtain the complete following discretization :

$$\begin{aligned}(12)\qquad &\frac{\hat{u}^{n+1}-\hat{u}^n}{\Delta t}+\frac{\sqrt{\nu}}{\sqrt{\Delta t}}\sqrt{\frac{3}{2}}\sum_{j=0}^{n} g_{n+1-j}\hat{u}^{j+\frac{1}{2}}\\ &\qquad = \hat{u}^{n+\frac{1}{2}}\left(-\alpha\xi^2 - i\xi + i\beta\xi^3\right) - \frac{i}{2}\gamma\xi\widehat{(u^n)^2},\end{aligned}$$

where $\hat{u}(t,\xi)$ denote the Fourier transform of $u(t,x)$.

3.2. The numerical results. In all the computations presented below, the initial data is $u_0(x) = 0.32{*}\mathrm{sech}^2(0.4{*}(x-x_0))$, where x_0 is the middle of the interval. This initial datum provides a small amplitude and long wave KdV soliton for $\alpha = \nu = 0$, $\beta = 1$ and $\gamma = 6$. Our aim is to compare our numerical results with those obtained in [7] in order to validate the use of a Gear operator for approximate a fractional derivative.

Remark on the stability : No attempt has been made to prove the convergence of the numerical scheme developed above. But when there is no viscosity, results exist in the literature on the stability of the scheme for a sufficiently small perturbation (see for example [16]). Using the data given above with a space step of discretization equal to $h = 0.2$, a numerical experiment shows that a time step of discretization equal to $\Delta t = 0.02$ is needed to ensure the stability on a time interval $[0,\ 100]$. These are the data considered in the computations.

But when the viscosity effects are taken into account, for example with a viscosity equal to $\nu = 0.1$, due to the diffusive property of this term, only a time step equal to $\Delta t = 0.2$ is required to ensure the stability on the time interval $[0, 100]$.

In Figure 1, we observe the effects of the local diffusion and non-local viscous terms in the linear case ($\gamma = 0$) for $(\alpha,\nu) = (0,1)$, $(\alpha,\nu) = (5,0)$ and $(\alpha,\nu) = (5,1)$, which correspond to cases with only non local viscous term, only local diffusion term and with both terms. The solutions are plotted at time $T = 100$.

We first note that when $(\alpha,\nu) = (0,0)$, the solution of the linear wave equation is a traveling wave with speed 1. So the solution at $T = 100$ would be the same shape of wave, but centered at 350. Comparing this with the case $(\alpha,\nu) = (0,1)$, we see that the non local viscous term slows the wave down significantly and also at the same time, enlarges the wave length. On the other hand, by comparing the cases $(\alpha,\nu) = (0,0)$ and $(\alpha,\nu) = (5,0)$, we see that the local diffusion term also enlarges the wave length, but preserves the velocity of the wave. When both viscous and diffusion terms are involved in the simulation, the wave profile is closer to the case with only local viscous term.

We now plan to observe numerically the results of Theorem 1 and obtain some quantitative insight on the decay of the solutions. Furthermore, we will investigate the cases where theoretical results are not available. For this purpose, we study the decay of the solutions for the L^∞ and the L^2 norm of (1), on the interval $(0, 1000)$,

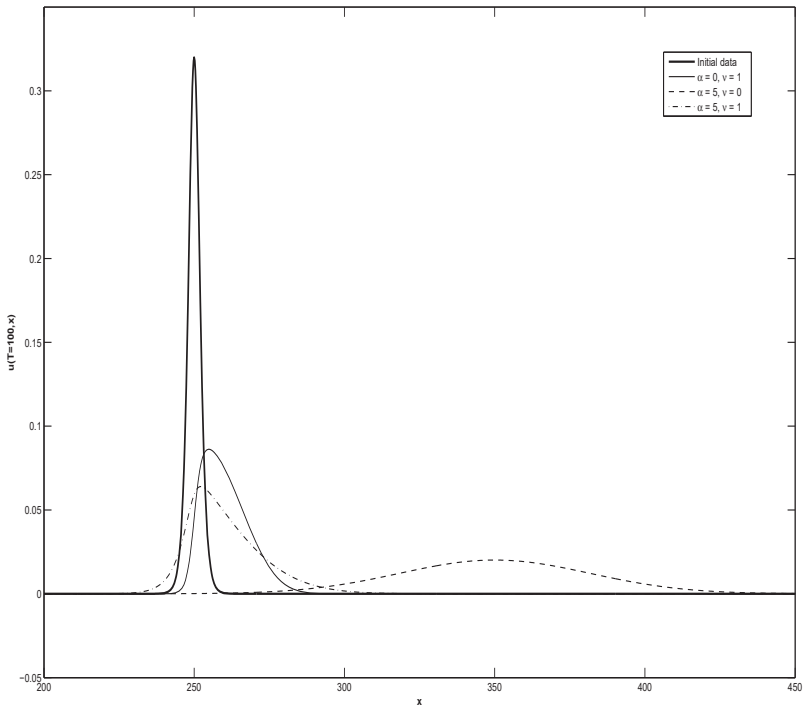

FIGURE 1. Solutions at time $T = 100$ for different viscosity (ν equal to 0 and 1, α equal to 0 and 5 and $\beta = \gamma = 0$).

when the viscosity coefficients $(\alpha, \nu) = (0, 0.1)$, $(0.1, 0)$ and $(0.1, 0.1)$, $\beta = 0$ and γ equal to 0 (linear) and 1 (nonlinear).

Since the expected decay is of the form $O(t^a)$, Figure 2 (resp. Figure 3) shows the ratio R_∞ (resp. the ratio R_2) versus the time t for the linear problem (γ equal to 0).

From Figure 2, one observes that the non local dissipative term produce a larger decay rate compared with the local dissipative term. The decay rates in all three cases appear to approach 0.5, but the convergence rate is quite small. The Figure 3 is for L^2-norm, instead of L^∞-norm and the result are similar. Similar computations are performed with $\gamma = 1$ (the nonlinear case).

We also compute the decay rate a for each of the two norms using the data from $[T - 200, T]$. The results are given in Table 2. These results match the theoretical results given in [7] (Theorem 1.4) for the cases where theoretical results are available. We can also observe that there is no significant difference between the linear and the non linear case. Moreover, the decay of the solution is the same when $\alpha = 0.1$ or $\nu = 0.1$.

TABLE 2. Decay rate of the solution $u(t, .)$ versus the time (ν and α equal to 0 and 0.1, $\beta = 0$, $\gamma = 0$ and 1).

Ratio	$(\alpha, \nu) = (0, 0.1)$		$(\alpha, \nu) = (0.1, 0)$		$(\alpha, \nu) = (0.1, 0.1)$	
	$\gamma = 0$	$\gamma = 1$	$\gamma = 0$	$\gamma = 1$	$\gamma = 0$	$\gamma = 1$
R_∞	-0.52	-0.52	-0.47	-0.49	-0.52	-0.52
R_2	-0.28	-0.28	-0.23	-0.24	-0.28	-0.28

Comparing these results with those obtained by [7], we can observe a difference of order 10^{-2} approximately between the two numerical methods. Thus we can say

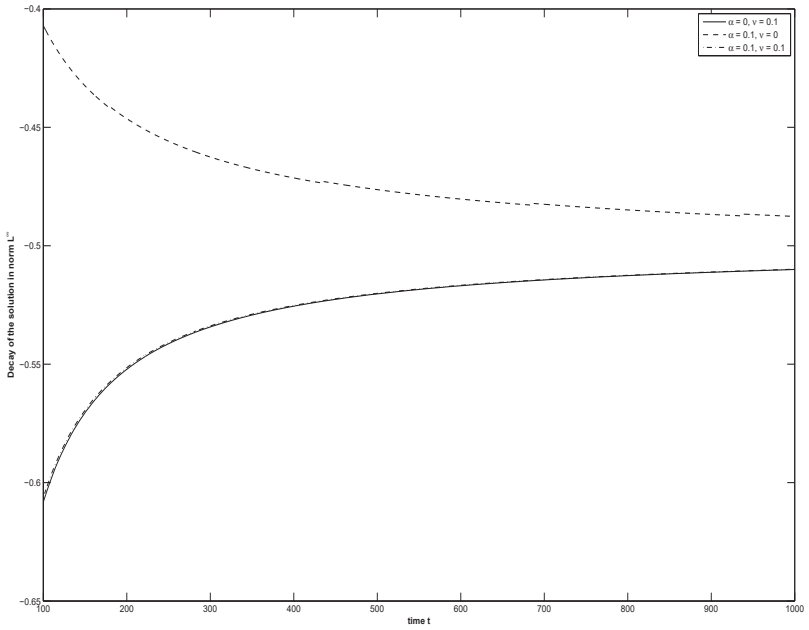

FIGURE 2. Ratio R_∞ versus the time ($(\alpha, \nu) = (0, 0.1)$, $(0.1, 0)$,$(0.1, 0.1)$, $\beta = 0$ and $\gamma = 0$). The first and the third curves overlap each other.

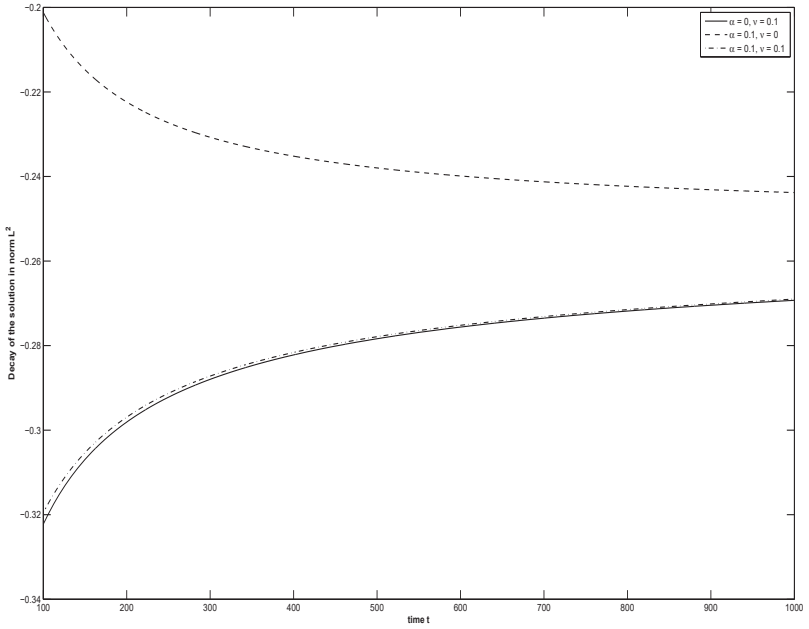

FIGURE 3. Ratio R_2 versus the time ($(\alpha, \nu) = (0, 0.1)$, $(0.1, 0)$,$(0.1, 0.1)$, $\beta = 0$ and $\gamma = 0$). The first and the third curves overlap each other.

that the use of the Gear operator to approximate a fractionnal derivative of order $\frac{1}{2}$ yields good results for these datasets.

In the final sequence of computations, we plan to study the different effects of diffusion and dispersion. We consider now the full equation (1), where the geometric dispersive term u_{xxx} plays a role. When there is no viscosity ($\alpha = \nu = 0$), the exact solution of the problem is the soliton $u(t, x) = u_0(x - 1.64 * t)$. In Figure 4, we compare solutions from (1) with different set of coefficients. The solutions with $(\alpha, \nu, \beta, \gamma) = (0, 0, 1, 6)$, *i.e.* KdV equation, $(\alpha, \nu, \beta, \gamma) = (0.1, 0, 1, 6)$, $(0, 0.1, 1, 6)$, $(0.1, 0.1, 1, 6)$ and the exact KdV solution are plotted. Again, the local dissipative

term slows the wave down. The local dispersive term might contribute to the appearance of the double hump.

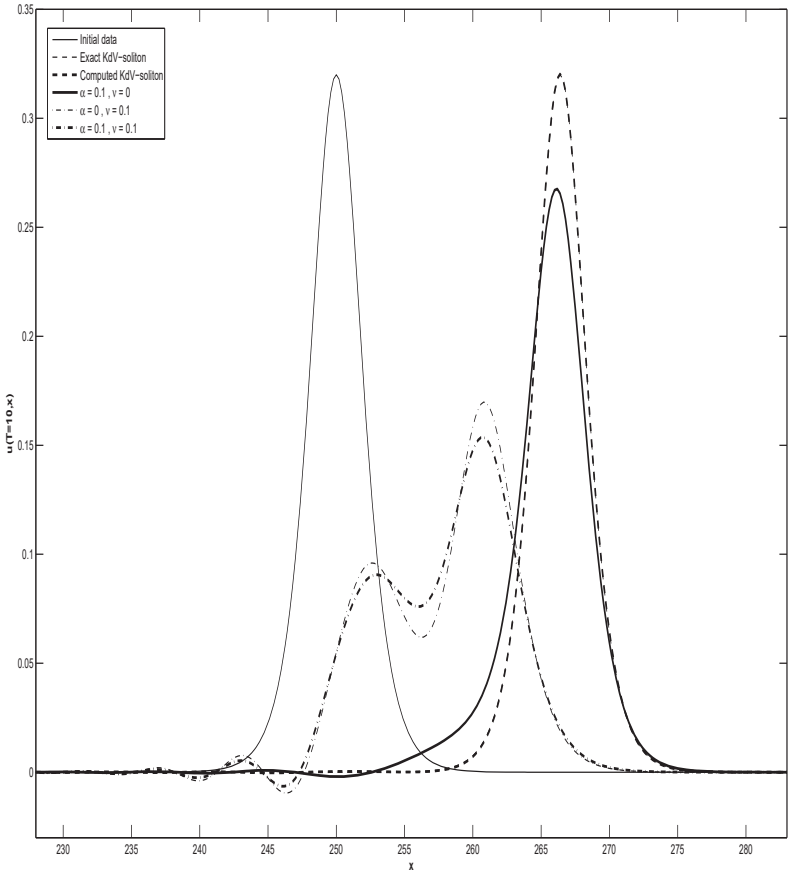

FIGURE 4. Solutions at time $T = 10$ (ν and α equal to 0 and 0.1, $\beta = 1$, $\gamma = 6$).

If we compare the Figure 4 to the Figure 5 in the article [7], we see that the computed solutions for these different coefficients are overall in the same form. But in using a Gear operator, we note an oscillatory effect more apparent than in [7].

We now investigate numerically the decay rate of the solutions when the local dispersion term u_{xxx} is present. For that we fix firstly β to 1 and γ to 6 and we vary the coefficients α and ν equal to 0 and 1. Finally we present the functions R_∞ and R_2 versus the time t in the Figure 5 and Figure 6.

As for Table 2, we computed the decay rate a of the solutions for these coefficients and these results are given in Table 3, and shows a decay rate near from $-\frac{1}{2}$ for the L^∞-norm and $-\frac{1}{4}$ for the L^2-norm.

TABLE 3. Decay rate of the solution $u(t,.)$ versus the time (ν and α equal to 0 and 1, $\beta = 1$, $\gamma = 6$).

Norm	$(\alpha,\nu) = (0,1)$	$(\alpha,\nu) = (1,0)$	$(\alpha,\nu) = (1,1)$
L^∞	-0.44	-0.51	-0.43
L^2	-0.23	-0.25	-0.22

To conclude this section, we can say that the results obtained by the Gear operator are analogous to those produced in [7]. Therefore the numerical method using the Gear operator turns out to be good technique to compute solutions of the equation (1).

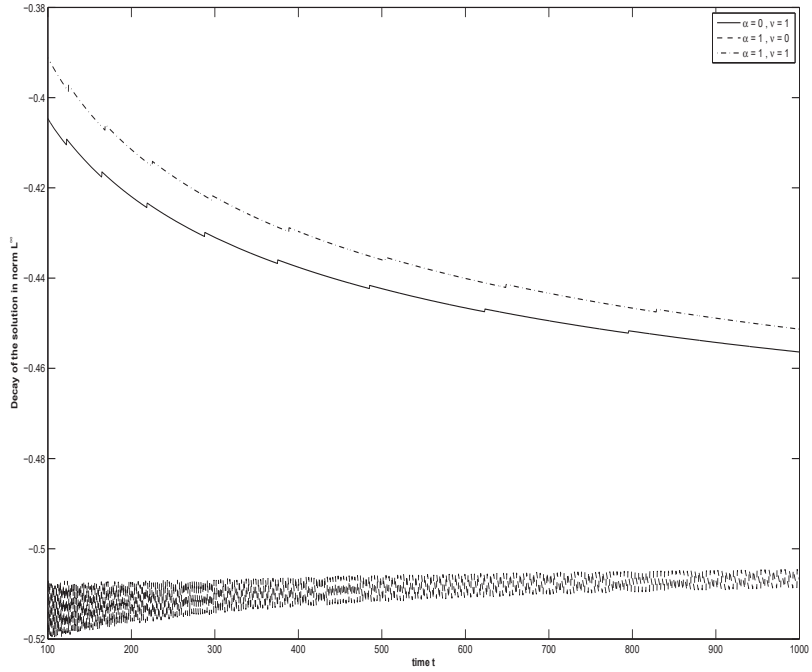

FIGURE 5. Ratio R_∞ versus the time (α and ν equal to 0 and 1, $\beta = 1$, $\gamma = 6$).

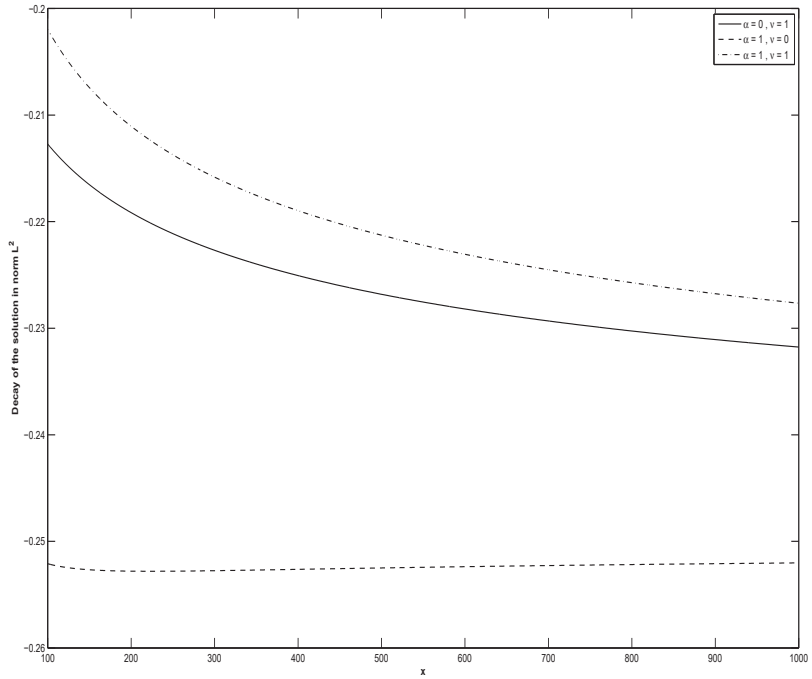

FIGURE 6. Ratio R_2 versus the time (α and ν equal to 0 and 1, $\beta = 1$, $\gamma = 6$).

4. Numerical study of the BBM-like equation

4.1. The numerical scheme. We describe in this section the numerical scheme to approximate solutions of (4).

For the time discretization, a semi-implicit Crank-Nicholson-leap-frog method (with the first step computed by a semi-implicit backward Euler method) is used in order to have a conservative scheme if $\alpha = \beta = \gamma = \nu = 0$ (for more details, see [6]). More precisely, let Δt be the time step and $t^n = n\Delta t$ for $n \in \mathbb{N}$, the scheme can be written, for $n \geqslant 1$

$$(13)\qquad \begin{aligned}(1-\beta\Delta)\,\frac{u^{n+1}-u^{n-1}}{2\Delta t}+\sqrt{\nu}\left(G^{\frac12}u\right)^n-\frac{\alpha}{2}\left(u_{xx}^{n+1}+u_{xx}^{n-1}\right)\\ +\frac12\left(u_x^{n+1}+u_x^{n-1}\right)+\gamma\frac12(u^n)_x^2=0,\end{aligned}$$

where u^n represents the numerical approximation of $u(t^n,.)$, and u^0 is the initial data u_0. The viscous term $\left(G^{\frac12}u\right)^n$ (see Section 2) at time t^n is approximated by

$$\begin{aligned}\left(G^{\frac12}u\right)^n&=\frac12 G^{\frac12}\left(u^{n+1}+u^{n-1}\right)\\&=\frac12\sqrt{\frac{3}{2\Delta t}}\left(\sum_{j=0}^{n+1}g_{n+1-j}u^j+\sum_{j=0}^{n-1}g_{n-1-j}u^j\right).\end{aligned}$$

For the space discretization, a Fourier discretization is implemented, so Fast Fourier Transforms can be used. Therefore, the periodic boundary condition on an interval $[0,L]$ with large L is used.

The fully discretized problem can be written, denoting by $\hat{u}(\xi)$ the Fourier transform of u at the frequency ξ, for $n\geq 1$

$$(14)\qquad \begin{aligned}(1+\beta\xi^2)\left(\hat{u}^{n+1}-\hat{u}^{n-1}\right)+\sqrt{\frac{3\nu\Delta t}{2}}\left(\sum_{j=0}^{n+1}g_{n+1-j}\hat{u}^j+\sum_{j=0}^{n-1}g_{n-1-j}\hat{u}^j\right)\\ +\Delta t\left(\alpha\xi^2+i\xi\right)\left(\hat{u}^{n+1}+\hat{u}^{n-1}\right)+i\gamma\Delta t\,\xi\hat{(u^n)}^2=0\end{aligned}$$

at time $t^n=n\Delta t$, and for $\xi=\frac{2\pi}{L}j$, $-\frac{N}{2}\leq j\leq\frac{N}{2}$ and N is the number of modes under consideration.

4.2. Validation of the scheme. In order to validate the numerical method used in the sequel, we will follow the ideas of M. Chen [6]. This technique consists in neglecting the viscous and viscous diffusion terms in equation (4), and compute numerically the solution of this equation with a known exact solitary-wave solution. With $\alpha=\nu=0$, $\beta=\gamma=1$, equation (4) reads

$$u_t+u_x-u_{txx}+uu_x=0.$$

Let $u(x,t)=\varphi(x-pt)$, φ satisfies

$$(p-1)\varphi'-p\varphi'''-\varphi\varphi'=0.$$

Using Lemma 1 in [5], namely $\alpha\eta'-\beta\eta'''-\eta\eta'=0$ admits a solution $\eta=3\,\alpha\,\mathrm{sech}^2\left(\frac12\sqrt{\frac{\alpha}{\beta}}x\right)$, one finds explicit solutions

$$(15)\qquad u(x,t)=\varphi(x-pt)=3\,(p-1)\,\mathrm{sech}^2\left(\frac12\sqrt{\frac{p-1}{p}}(x-pt)\right).$$

The one with $p=2$ is used for our test.

For an interval of length $L=400$ with $N=800$ modes, a time step $\Delta t=0.01$, the computed solution has $\|u(T,.)\|_{L^\infty}$ equal to 3.00005 at time $T=50$ while the explicit solution has $\|u_{\mathrm{ex}}(T,.)\|_{L^\infty}$ equal to 3. The maximum difference between the computed solution $u(T,.)$ and $u_{\mathrm{ex}}(T,.)$ at $T=50$, $\|u_{\mathrm{ex}}(T,.)-u(T,.)\|_{L^\infty}$ is equal to 3.05×10^{-4}. By halving the size of $\Delta t=0.005$, $\|u_{\mathrm{ex}}(T,.)-u(T,.)\|_{L^\infty}$ decreased to 7.6×10^{-5}. Therefore, the numerical scheme is validated for non-dissipative

equation and it is second order in time as expected. It has a spectral accuracy in space.

4.3. Solutions and decay rate for various values of the parameters. In the first part of this section, we show the influence of parameters α, β, γ and ν on the solutions. These computations are realized on the interval $[0, L]$ with $L = 800$. The space step size h is equal to $h = 0.1$ and the time step size Δt is equal to $\Delta t = 0.1$ The initial datum is the function $u(x, t = 0)$ defined in (15) with $p = 2$ and has the peak at shifted $x_0 = 100$.

Figure 7, Figure 8 and Figure 9 show the solutions for various values of the parameters α, β, γ and ν at time $T = 500$.

In Figure 7, we can observe that the non local viscous term ν slows the wave down significantly. We note also the influence of this parameter, since the wave profiles are very close to some of the other, despite a change of values of the other coefficients. The influence of viscous term will be studied more precisely in the sequel.

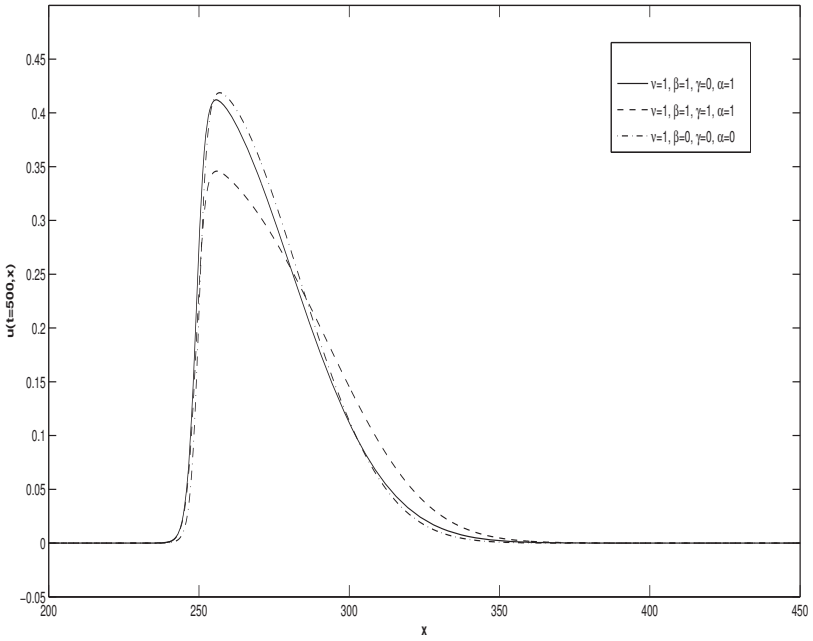

FIGURE 7. Solutions for α, β, γ equal to 0 or 1 ($\nu = 1$).

We observe in Figure 8 that the wave moves faster than in the case $\nu = 1$, but have their wave lengths expanded and their amplitude reduced. We also note that the solutions for $\nu = 0$, $\alpha = \gamma = 1$ are very similar and consequently the parameter β does not play an important role in this simulation. On the other side, the nonlinear term γ might contribute to the general form of the solution, because Figure 8 shows that if $\gamma = 1$, the appearance of the wave is more leaning toward the right, while for $\gamma = 0$, the wave is centered at $x = 600$.

In Figure 9, we have plotted solutions for different values of the parameters. We observe the same graphs obtained in Figure 7 when the parameter $\nu = 1$. On the other side, for $\nu = 0.1$, the solution is more damped than for the two other solutions, but also its wave length is larger.

Numerical simulations are performed to compute the decay rates of solutions obtained above for various values of parameters, both with the L^2 and L^∞-norm.

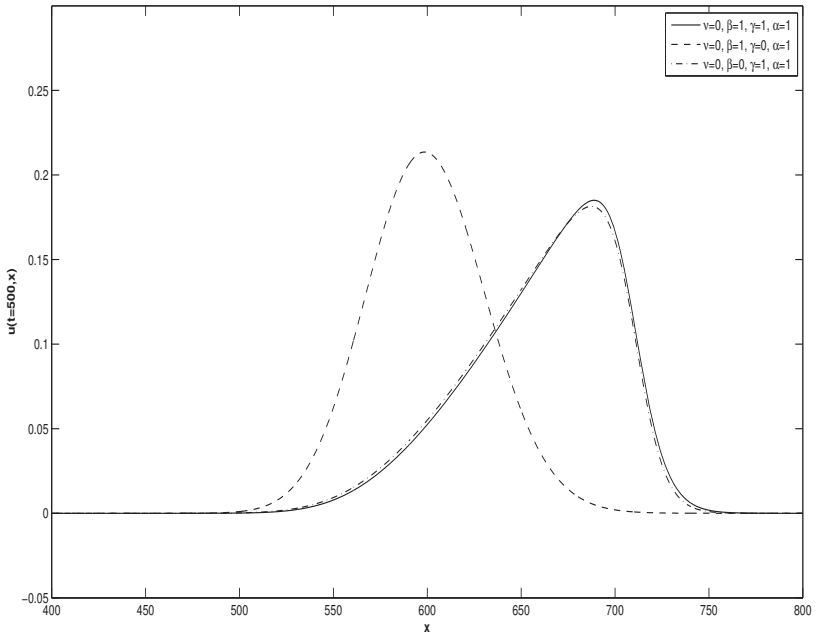

FIGURE 8. Solutions for α, β, γ equal to 0 or 1 ($\nu = 0$).

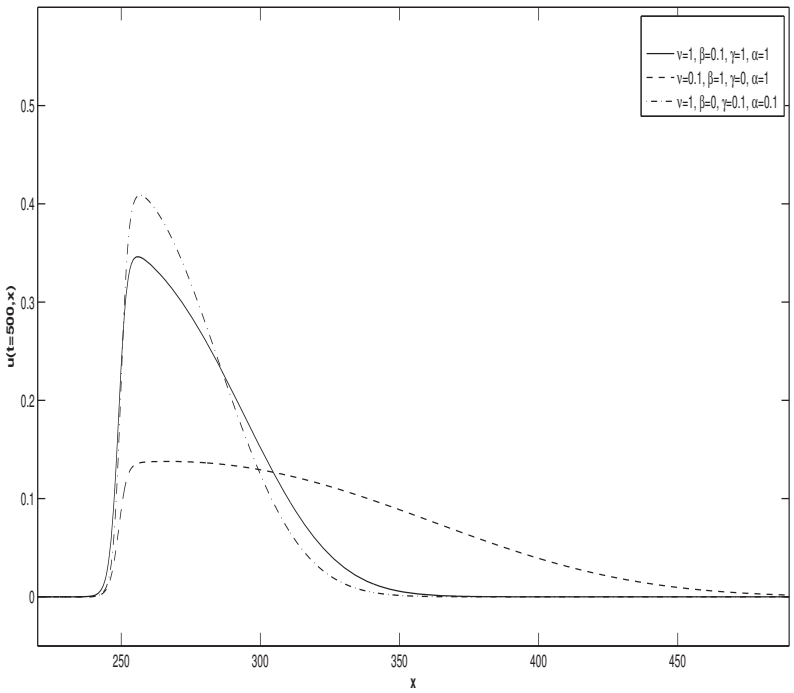

FIGURE 9. Solutions for α, β, γ and ν equal to $0, 0.1$ or 1.

For this computation, the domain of computation, the space step and time of discretization and the initial datum remain unchanged.

The functions R_2 and R_∞ versus the time t are plotted in Figure 10 and 11 for $\nu = 1$, Figure 12 and 13 for various values of parameters. The values of the decay rate are presented in Table 4. Looking more closely at these results on the decay rates, there is a certain similarity with the results for equation (1). That is to say, when the non local viscosity occurs, the decay rate are around -0.24 for the L^2-norm as in equation (1) and are around -0.48 for the L^∞-norm. We can say that both solutions of KdV and BBM equations with the non local viscosity term have nearly the same decay rate.

TABLE 4. Decay rate of the solution $u(t,.)$ versus the time for various values of the parameters.

Viscosity ν	Dispersive term β	Non linear term γ	Diffusion term α	L^2 decay rate	L^∞ decay rate
1	1	0	1	-0.22	-0.45
1	1	1	1	-0.20	-0.40
1	0	0	0	-0.24	-0.48
0	1	1	1	-0.25	-0.52
0	1	0	1	-0.25	-0.49
0	0	1	1	-0.25	-0.50
1	0.1	1	1	-0.20	-0.39
0.1	1	0	1	-0.28	-0.54
1	0	0.1	0.1	-0.23	-0.46

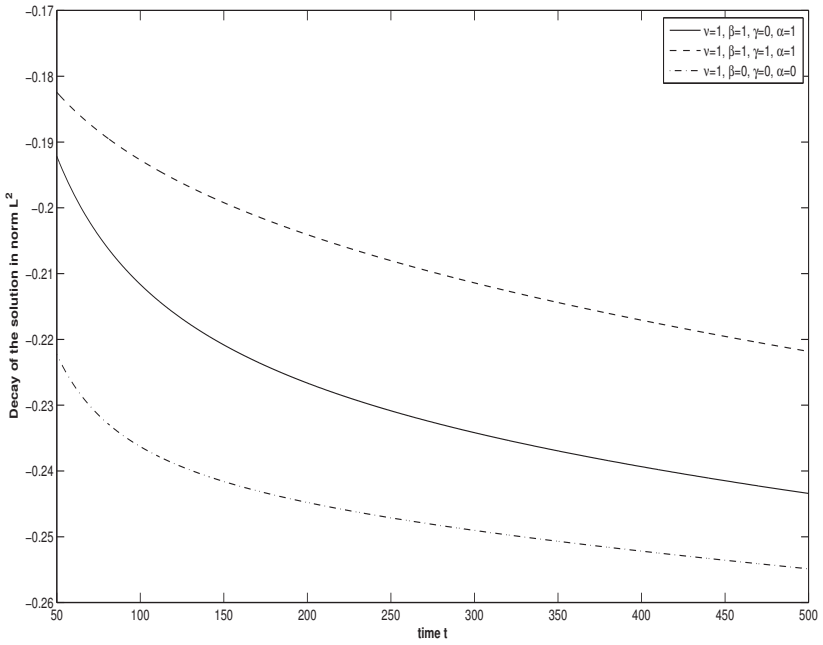

FIGURE 10. Ratio R_2 versus the time t for α, β, γ equal to 0 or 1 ($\nu = 1$).

4.4. Influence of the magnitude of the viscosity. In this subsection, numerical experiments are performed to study the influence of the viscosity on the decay rate. In these computations, the data are: $L = 2000$, $h = 0.2$, $\Delta t = 0.2$, $T = 1000$, $\alpha = 0$ and $\beta = \gamma = 1$. In these experiments, the initial datum is the function (15) with $p = 2$, and shift around the point $x_0 = L/2$.

The solutions at $T = 1000$ for equations with various ν between 0.1 and 20 are plotted in Figure 14. As expected, we observe that the viscosity increases the damping of the wave. In addition, the velocity of the wave also decreases with the viscosity.

The ratio R_2 and R_∞ versus the time t are plotted in Figure 15 and 16 for different values of ν. The values of decay rate are shown in Table 5. We notice immediately in Table 5 the influence of viscosity, because the more the values of ν increases, the more the value of decay rate in L^2 and L^∞-norm decreases. This results are consistent with comments made on the Figure 14.

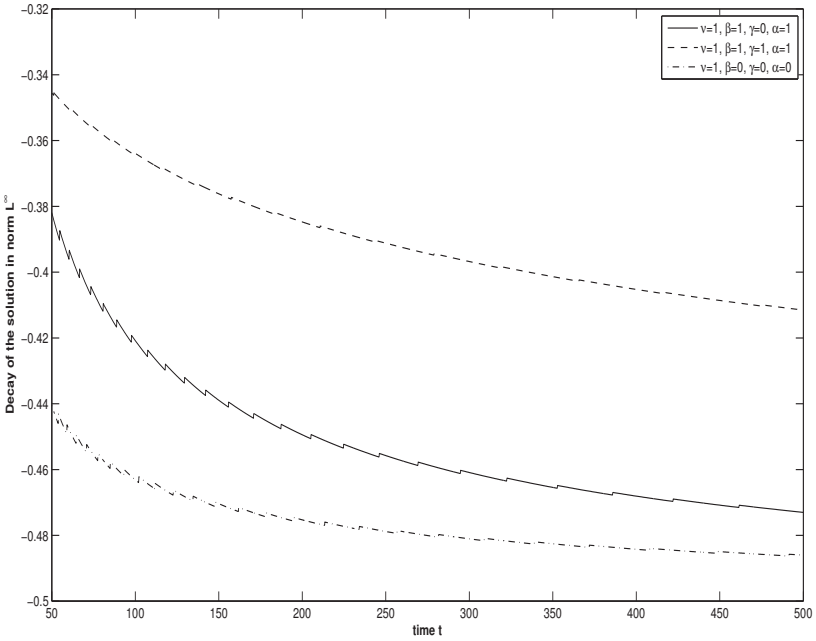

FIGURE 11. Ratio R_∞ versus the time t for α, β, γ equal to 0 or 1 ($\nu = 1$).

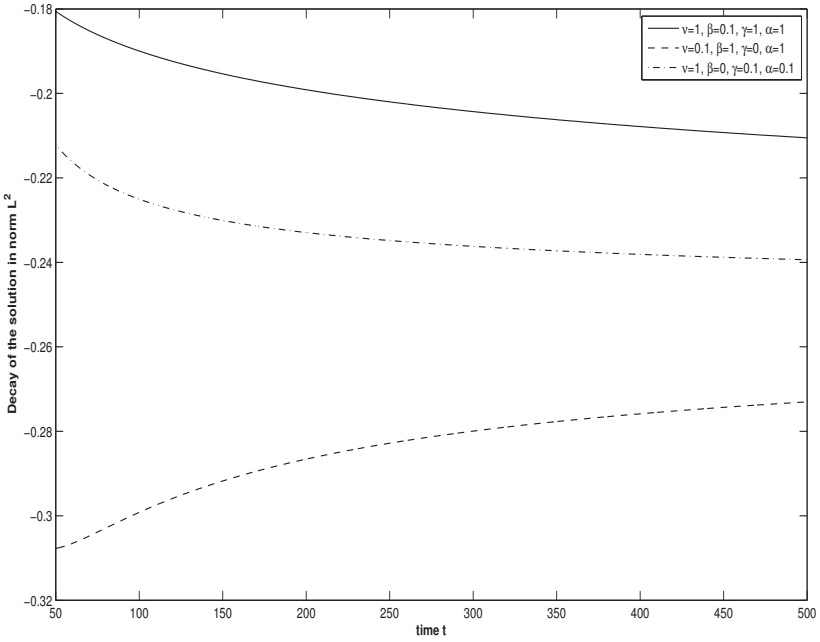

FIGURE 12. Ratio R_2 versus the time t for α, β, γ and ν equal to $0, 0.1$ or 1.

5. Conclusion

In this paper, we propose a discretization of the non local viscosity using a G^α-scheme. The technique permits us to study the influence of the viscosity on the decay rate for the viscous KdV-like equation and compare these results to those obtained in [7]. Moreover, a study of the influence of the viscosity on the viscous BBM-like equation is presented, study that can not be allowed using techniques developed in [7].

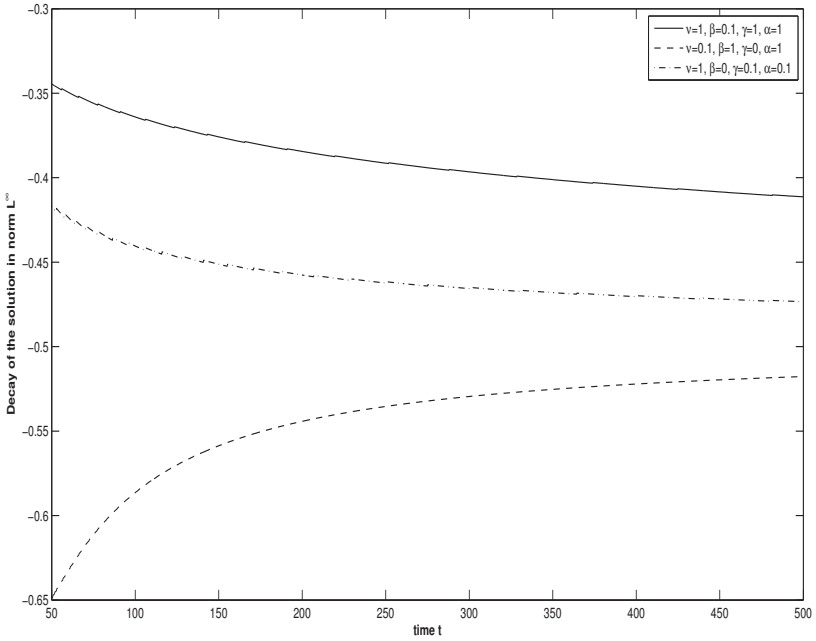

FIGURE 13. Ratio R_∞ versus the time t for α, β, γ and ν equal to $0, 0.1$ or 1.

TABLE 5. Decay rate of the solution $u(t,.)$ versus the time for various values of ν ($\beta = \gamma = 1$ and $\alpha = 0$).

Viscosity ν	L^2 decay rate	L^∞ decay rate
0.1	-0.26	-0.47
0.5	-0.23	-0.43
1	-0.21	-0.41
2	-0.20	-0.39
5	-0.18	-0.35
10	-0.17	-0.32
20	-0.15	-0.30

References

[1] C. J. Amick, J. L. Bona and M. E. Schonbek, *Decay of solutions of some nonlinear wave equations*, J. Differential Equations, **81** (1989), pp. 1-49.

[2] J. L. Bona, M. Chen and J.-C. Saut, *Boussinesq equations and other systems for small-amplitude long waves in nonlinear dispersive media, I, Derivation and the linear theory*, J. Nonlinear Sci., **12**, 2002, pp. 283-318.

[3] J. L. Bona, F. Demengel and K. Promislow, *Fourier splitting and dissipation of nonlinear dispersive waves*, Proc. Roy. Soc. Edinburgh Sect. A 129 (1999), No. 3, pp. 477-502.

[4] J. L. Bona, K. Promislow and C. E. Wayne, *Higher-order asymptotics of decaying solutions of some nonlinear, dispersive, dissipative wave equations*, Nonlinearity 8 (1995), No. 6, pp. 1179-1206.

[5] M. Chen, *Exact Traveling-wave solutions to bi-directional wave equations*, International Journal of Theoretical Physics, vol. **37**, Number 5, 1998, pp. 1547-1567.

[6] M. Chen, *Numerical investigation of a two-dimensional Boussinesq system*, Discrete Contin. Dyn. Syst., Vol **28**, 2009, No. 4, pp. 1169-1190.

[7] M. Chen, S. Dumont, L. Dupaigne and O. Goubet, *Decay of solutions to a water wave model with a nonlocal viscous dispersive term*, Discrete Contin. Dyn. Syst., **27**, 2010, No. 4, pp. 1473-1492.

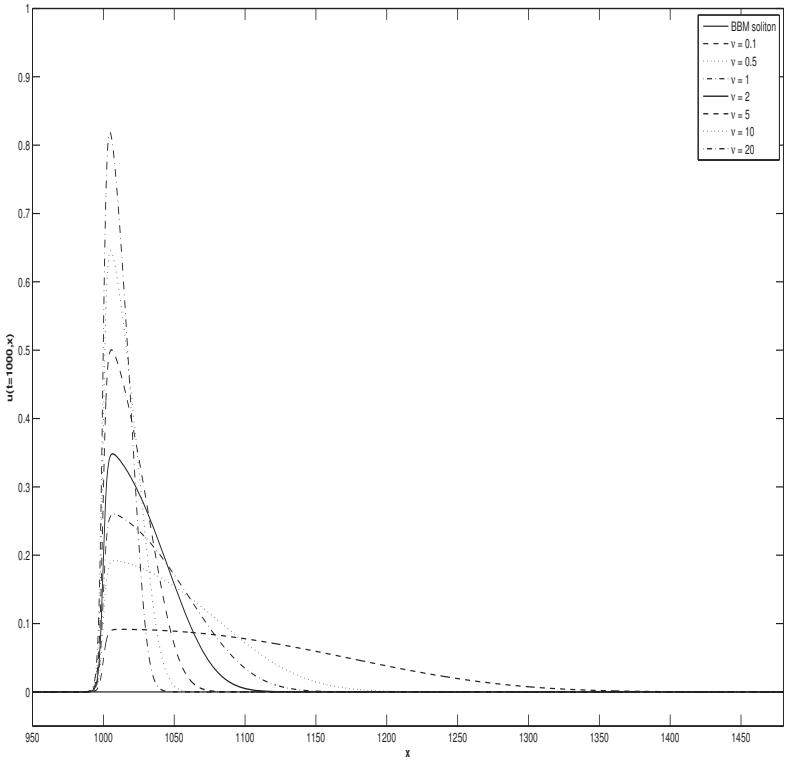

FIGURE 14. Solutions for the viscosity ν ranging from 0.1 to 20.

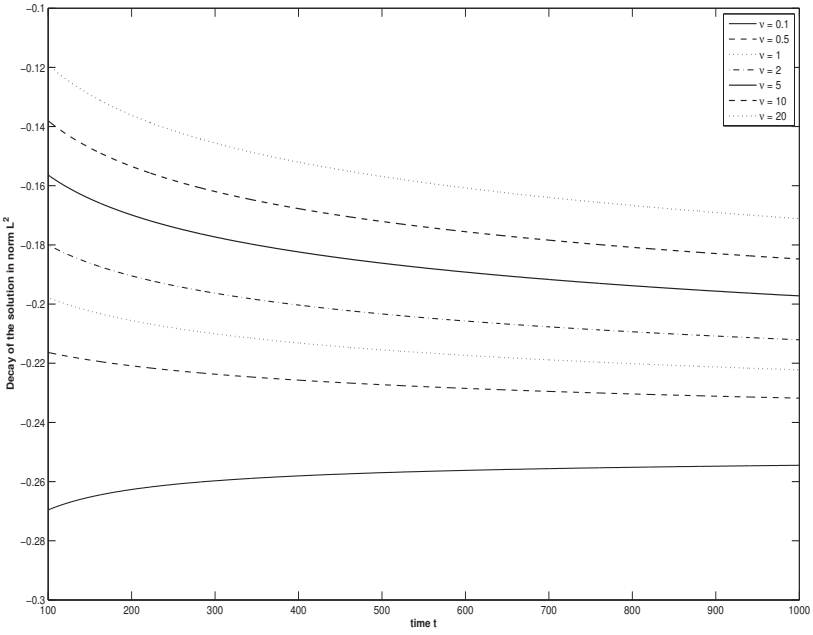

FIGURE 15. Ratio R_2 versus the time t for ν ranging from 0.1 to 20.

[8] M. Chen and O. Goubet, *Long-Time Asymptotic Behavior of 2D Dissipative Boussinesq System*, Discrete Contin. Dyn. Syst., Vol. **17**, Number 3, 2007, pp. 509-528.

[9] A.-C. Galucio , J.-F. Deü, S. Mengué and F. Dubois, *An adaptation of the Gear scheme for fractionnal derivatives*, Comput. Methods Appl. Mech. Engrg., 195(2006), pp. 6073-6085.

[10] F. Dubois, A.-C. Galucio and N. Point, *Introduction à la dérivation fractionnaire - Théorie et Applications*, `http://www.math.u-psud.fr/fdubois/travaux/evolution/ananelly-07/techinge08/techinge-01nov08.pdf`.

[11] D. Dutykh, *Visco-potential free-surface flows and long wave modeling*, European Journal of Mechanics B/Fluids, **28**(3), 2009, pp. 430-443.

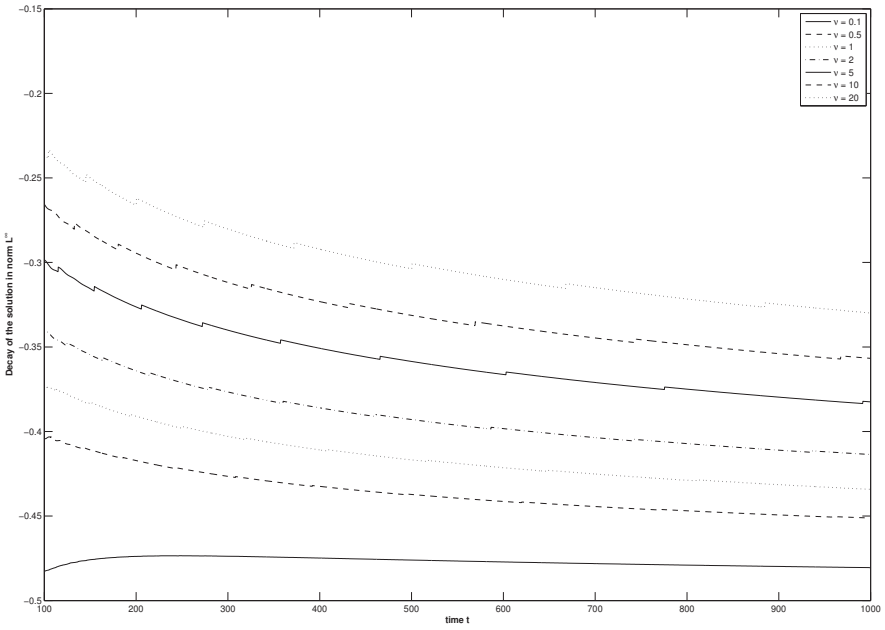

FIGURE 16. Ratio R_∞ versus the time t for ν ranging from 0.1 to 20.

[12] D. Dutykh and F. Dias, *Viscous potential free-surface flows in a fluid layer of finite depth*, C. R. Math. Acad. Sci. Paris, **345**, 2007, pp. 113-118.

[13] O. Goubet and G. Warnault, *Decay of solutions to a linear viscous asymptotic model for water waves*, Chin. Ann. Math. Ser. B, Vol. 31, No. 6, 2010, pp. 841-854.

[14] T. Kakutani and K. Matsuuchi, *Effect of viscosity of long gravity waves*, J. Phys. Soc. Japan, **39**, 1975, pp. 237-246.

[15] P. Liu and A. Orfila, *Viscous effects on transcient long-wave propagation*, J. Fluid Mech., **520**, 2004, pp. 83-92.

[16] K. Pen-Yu, J. M. Sanz-Serna, *Convergence of methods for the numerical solution of the Korteweg-de-Vries equation*, IMA Journal of Numerical Analysis, **1** (1981), 215-221.

LAMFA CNRS UMR 7352, Université de Picardie Jules Verne, 33, rue Saint-Leu, 80039 Amiens, France.

E-mail: `serge.dumont@u-picardie.fr`

URL: `http://lamfa.u-picardie.fr/dumont/`

LMAC EA 2222, Université de Technologie de Compiègne, Centre de Recherches de Royallieu, 60205 Compiègne, France.

E-mail: `jean-baptiste.duval@u-picardie.fr`

URL: `http://lamfa.u-picardie.fr/duval`